Broadening the spectrum of Ehlers Danlos syndrome in patients with congenital adrenal hyperplasia

Rachel Morissette[1]*, Wuyan Chen[2]*, Ashley F. Perritt[1], Jennifer L. Dreiling[3], Andrew E. Arai[4], Vandana Sachdev[4], Hwaida Hannoush[4], Ashwini Mallappa[1], Zhi Xu[5], Nazli B. McDonnell[5], Martha Quezado[3], Deborah P. Merke[1,6]

[1] National Institutes of Health, Clinical Center, Bethesda, MD, USA; [2]PreventionGenetics, Marshfield, WI, USA; [3]Laboratory of Pathology, National Cancer Institute, Bethesda, MD, USA; [4]National Institute of Heart, Lung, and Blood, Bethesda, MD USA; [5]National Institutes of Health, National Institute on Aging, Baltimore, MD, USA; [6] The *Eunice Kennedy Shriver* National Institute of Child Health and Human Development, Bethesda, MD, USA
Clinical Trial Registration Number: ClinicalTrials.gov Identifier #NCT00250159

Context: The contiguous gene deletion syndrome, CAH-X, was described in a subset (7%) of congenital adrenal hyperplasia (CAH) patients with a *TNXA/TNXB* chimera resulting in deletions of *CYP21A2*, encoding 21-hydroxylase necessary for cortisol biosynthesis, and *TNXB*, encoding the extracellular matrix glycoprotein tenascin-X (TNX). This *TNXA/TNXB* chimera is characterized by a 120 bp deletion in exon 35 and results in *TNXB* haploinsufficiency, disrupted transforming growth factor-β (TGF-β) signaling, and an Ehlers Danlos syndrome (EDS) phenotype.

Objective: To determine the genetic status of *TNXB* and resulting protein defects in CAH patients with a CAH-X phenotype but not the previously described *TNXA/TNXB* chimera.

Design, Settings, Participants, Intervention: A total of 246 unrelated CAH patients were screened for *TNXB* defects. Genetic defects were investigated by Southern blotting, multiplex ligation-dependent probe amplification, Sanger, and next-generation sequencing. Dermal fibroblasts and tissue were used for immunoblotting, immunohistochemical, and co-immunoprecipitation experiments.

Main Outcome Measures: The genetic and protein status of tenascin-X in phenotypic CAH-X patients.

Results: Seven families harbor a novel *TNXB* missense variant c.12174C>G (p.C4058W) and a clinical phenotype consistent with hypermobility-type EDS. Fourteen CAH probands carry previously described *TNXA/TNXB* chimeras and 7 unrelated patients carry the novel *TNXB* variant resulting in a CAH-X prevalence of 8.5%. This highly conserved pseudogene-derived variant in the TNX fibrinogen-like domain is predicted to be deleterious and disulfide bonded, results in reduced dermal elastin and fibrillin-1 staining and altered TGF-β1 binding, and represents a novel *TNXA/TNXB* chimera. Tenascin-X protein expression was normal in dermal fibroblasts, suggesting a dominant negative effect.

Conclusions: CAH-X syndrome is commonly found in CAH due to 21-hydroxylase deficiency and may result from various etiological mechanisms.

Abbreviations:

A deficiency in 21-hydroxylase (encoded by *CYP21A2*) leads to congenital adrenal hyperplasia (CAH, OMIM 201 910), an autosomal recessive disorder of the adrenal cortex characterized by cortisol deficiency, with or without aldosterone deficiency, and androgen excess, the severity of which depends on the degree of 21-hydroxylase impairment (1). The severe or classic form is a rare orphan disease occurring in 1 in 16 000 live births, while the mild or nonclassic form is estimated to occur in 1 in 1000 people (2). Flanking *CYP21A2* is the *TNXB* gene encoding tenascin-X (TNX), an extracellular matrix (ECM) glycoprotein that is highly expressed in connective tissue. TNX plays a role in collagen fibrillogenesis and matrix maturation, though it functions in collagen fibril deposition independent of collagen synthesis (3). Normal collagen fibril deposition in connective tissue is essential for the collagenous matrix integrity and defects lead to Ehlers Danlos syndrome (EDS), a hereditary connective tissue disorder (4). Complete TNX deficiency was first reported in a patient with CAH and EDS (5). While autosomal recessive complete TNX deficiency is a cause of classical EDS (OMIM 130 000), (6) *TNXB* haploinsufficiency is associated with hypermobile EDS (OMIM 130 020), (7) and when present in patients with CAH, results in a contiguous gene deletion syndrome termed CAH-X (8).

The *CYP21A2* (OMIM 201 910) and the *TNXB* (OMIM 600 985) genes reside in tandem on chromosome 6p23.1 within the human leukocyte antigen histocompatibility complex in a module characterized by highly homologous sequences between functional genes (*CYP21A2* and *TNXB*) and their corresponding pseudogenes (*CYP21A1P* and *TNXA*), which leads to frequent homologous recombination. Chimeric genes generated by large gene deletion or gene conversion events, account for 20%–30% of the common *CYP21A2* pathogenic variants in 21-hydroxylase-deficient patients (9–11). To date, 9 *CYP21A2/CYP21A1P* (CH-1 to CH-9) and one *TNXA/TNXB* chimera (termed CH-1 here) have been described (5, 11). The previously described *TNXA/TNXB* CH-1 results in a contiguous *CYP21A2* and *TNXB* deletion found in 7% of CAH patients, and has been estimated to account for 13% of large *CYP21A2* deletions (8). *TNXA/TNXB* CH-1 is characterized by a 120 bp deletion crossing exon 35 and intron 35 carried over from the *TNXA* pseudogene; this is the only well-documented discrepancy between *TNXB* and *TNXA*.

The TNX protein is divided into an N-terminal signal peptide, followed by TNX assembly, epidermal growth factor (EGF)-like, fibronectin type III, and C-terminal fibrinogen-like domains (12). All but one previously reported TNX genetic defects are in the fibronectin type III domains (13–15). Though the exact mechanism behind TNX's ability to organize the ECM is unknown, the TNX fibrinogen-like domain activates the transforming growth factor-β (TGF-β) pathway, a regulator of collagen production important in connective tissue dysplasias (16). Additionally, we recently showed aberrant TGF-β signaling in patients with CAH-X syndrome (17).

In this study, we evaluated the *TNXB* gene and the TNX protein in CAH patients with a CAH-X phenotype who did not have the previously described *TNXA/TNXB* CH-1. Since the junction site of a chimeric *TNXA/TNXB* gene theoretically can be anywhere between exons 32 through 44 (the homologous region), we hypothesized that novel *TNXA/TNXB* chimeras might exist. Our study provides functional evidence of a novel *TNXA/TNXB* chimera resulting in CAH-X syndrome, thereby broadening the genetic and phenotypic spectrum of CAH due to 21-hydroxylase deficiency.

Materials and Methods

Study Subjects

In a large prospective cohort of 246 unrelated patients (146 females, aged 1–65 years) with CAH due to 21-hydroxylase deficiency, we studied patients with a phenotype suspicious for CAH-X syndrome. Patients were enrolled in an ongoing prospective natural history study at the National Institutes of Health Clinical Center in Bethesda, MD (Clinical Trials # NCT00250159) and approval was obtained from the *Eunice Kennedy Shriver* National Institute of Child Health & Human Development Institutional Review Board. Written informed consent was obtained from all participants and parents of participating children. All minors at least 8 years old gave assent. The diagnosis of 21-hydroxylase deficiency was determined by hormonal evaluation (17-hydroxyprogesterone > 1200 ng/dL) and *CYP21A2* genotyping (18). Previously reported subjects with CAH-X syndrome due to *TNXB* haploinsufficiency (14 probands, 16 related patients) and CAH controls were used as comparison groups (8).

All patients were evaluated prior to genotyping for joint hypermobility using the Beighton 9-point scale and for major and minor criteria of classical and hypermobile EDS as previously described (8). Generalized hypermobility was determined by an individual's age and Beighton score and defined as ≥ 5 for children and ≥ 4 for postpubertal adolescents and adults (19). Skin characteristics were evaluated, including extensibility, thinness, scar formation, and striae. Transthoracic 2-dimensional echocardiography and magnetic resonance imaging (MRI) of the heart (1.5 T scanner) were performed in patients with a CAH-X phenotype and their relatives when possible.

Genetic Analysis

Sanger sequencing (*CYP21A2* and *TNXB* genes) and next-generation sequencing (EDS panel: *COL3A1*, *COL5A1*, *COL5A2* genes) were performed in a commercial diagnostics laboratory (PreventionGenetics, Marshfield, WI, USA). The

amino acid substitution prediction programs PolyPhen-2 and SIFT were used to predict missense variant pathogenicity (12, 13). Multiplex ligation-dependent probe amplification (MLPA) and Southern blotting were done as previously described (8, 20). Two hundred healthy subjects (Coriell Repository, http://ccr.coriell.org) served as controls for evaluating allele frequency in the general population. All new *TNXB* variants described were submitted to the ClinVar database (http://www.ncbi.nlm.nih.gov/clinvar/).

Tenascin-X Modeling and Disulfide Prediction

The primary sequence of the tenascin-X C-terminal fibrinogen-like domain, corresponding to residues 4023–4233, was submitted to the Robetta server (http://www.robetta.org) for domain (Ginzu) (21) and tertiary structure predictions (Rosetta) (22, 23). The disulfide bonding state of C4058 was analyzed by submitting the C-terminal fibrinogen-like domain to several university-based online disulfide bonding state predictors (http://bioserv.rpbs.jussieu.fr/cgi-bin/CysState) (24, 25).

Fibroblast Cell Culture

Primary skin fibroblasts were initiated from 3 mm-punch biopsy explants from 7 CAH patients with the novel *TNXB* variant and 10 age- and sex-matched CAH controls with a normal *TNXB* genotype. Fibroblasts from second through third passages were cultured to confluence in high glucose Dulbecco's modified Eagle's medium (DMEM, Invitrogen, Carlsbad, CA, USA), 10% fetal bovine serum, penicillin, and streptomycin (Invitrogen) at 37°C in 5% CO_2.

Western Blot Analysis

Protein expression was analyzed by SDS-PAGE and western blot as previously described (17) with the following changes: 10 μg protein was loaded onto a 3%–8% NuPAGE Novex Tris-acetate precast gel (Invitrogen) and immunoblotting was done using a rabbit polyclonal antihuman tenascin-X (H-90) antibody (1:200; Santa Cruz Biotechnology, Santa Cruz, CA, USA) or rabbit polyclonal antihuman β-tubulin antibody (1:2000; Cell Signaling Technology, Danvers, MA, USA) overnight at 4°C. Secondary antibody incubation, blot visualization, and quantification were done as previously described (17). All data were normalized to the loading control. Experiments were performed in triplicate.

Elastin and Fibrillin-1 Staining in Dermal Biopsies

Five-micrometer sections of paraffin-embedded skin biopsies were mounted on Superfrost Plus slides (Erie Scientific, Portsmouth, NH, USA) and sections were stained with hematoxylin and eosin (H&E) using a Leica CV5030 Autostainer (Leica, Buffalo Grove, IL, USA).

Elastin-Van Gieson (EVG) staining of elastic fibers was done using an Artisan Multistainer (DakoCytomation, Carpinteria, CA, USA) and Dako Artisan staining reagents (Artisan EVG Kit, DakoCytomation). The epidermal layer served as an internal negative control for each skin biopsy.

Mouse antifibrillin-1 monoclonal antibody clone 26 (EMD Millipore, #MAB2502, Billerica, MA, USA) was used at a 1:300 dilution. Automated Leica BOND-MAX and its detection kit (Leica Biosystems, Bannockburn, IL, USA) were used for anti-fibrillin-1 immunohistochemical staining. Primary antibody was incubated for 30 minutes, polymer and postpolymer for 15 minutes, 3,3′-diaminobenzidine chromogen for 10 minutes, and hematoxylin for 5 minutes. Negative controls were done likewise but used mouse serum without primary antibody. Slides were viewed at 200x magnification.

Co-Immunoprecipitation

Coimmunoprecipitation experiments were conducted according to Alcaraz, et al (16) Briefly, whole cell lysate (equivalent volume of 10 ug protein according to a BCA assay) from dermal fibroblasts was lysed as above and subjected to immunoprecipitation using the Dynabeads Protein G Immunoprecipitation Kit (Invitrogen) according to the manufacturer's instructions. A purified rat anti-Mouse, Human, Pig TGF-β1 antibody (BD Biosciences, San Jose, CA, USA) was used to pull-down and Normal Rat IgG (R&D Systems, Minneapolis, MN, USA) antibody was used as a control for nonspecific binding. The entire eluates from the Dynabeads kit were loaded onto the gel and subjected to SDS-PAGE and western blotting with an anti-tenascin-X antibody as described above.

Statistical Analysis

Comparisons were made using the unpaired Student's *t* test. (Microsoft Excel). P-values are two-tailed and considered significant when ≤ 0.05. Data are represented as mean $\pm$ standard error of the mean (SEM).

Results

Novel *TNXB* Variant c.12174C>G Associated with CAH-X

Ten phenotypic CAH-X patients from 7 families were heterozygous for the novel *TNXB* missense variant in exon 40 defined as c.12174C>G (**Figure 1A**), which is predicted to result in the amino acid substitution p.C4058W within the TNX C-terminal fibrinogen-like domain. The prediction programs PolyPhen-2 and SIFT predicted that the p.C4058W change to be "probably damaging" and "deleterious", respectively. This variant was not found in 200 healthy subjects. In our cohort, 14 CAH probands carry previously described *TNXA*/*TNXB* chimeras and 7 unrelated patients carry the novel *TNXB* variant resulting in a CAH-X prevalence of 8.5%.

All 10 CAH patients with the c.12174C>G variant had EDS clinical features (Table 1). Generalized joint hypermobility, a major diagnostic criterion for classical EDS, was found in all patients. Hypermobility of small (**Figure 1B-1**) and large joints (**Figure 1B-2**) and hernias (**Figure 1B-3**) were found in 4 (40%), 7 (70%), and 3 (30%) patients, respectively. Most adults (90%) had chronic arthralgia in 4 or more joints. Other characteristic CAH-X clinical findings included structural cardiac abnormalities, elongated uvula with midline crease, and piezogenic pedal papules. Unlike the previously-reported CAH-X CH-1 patients, a subset of patients with the novel c.12174C>G variant had skin laxity (40%). The clinical
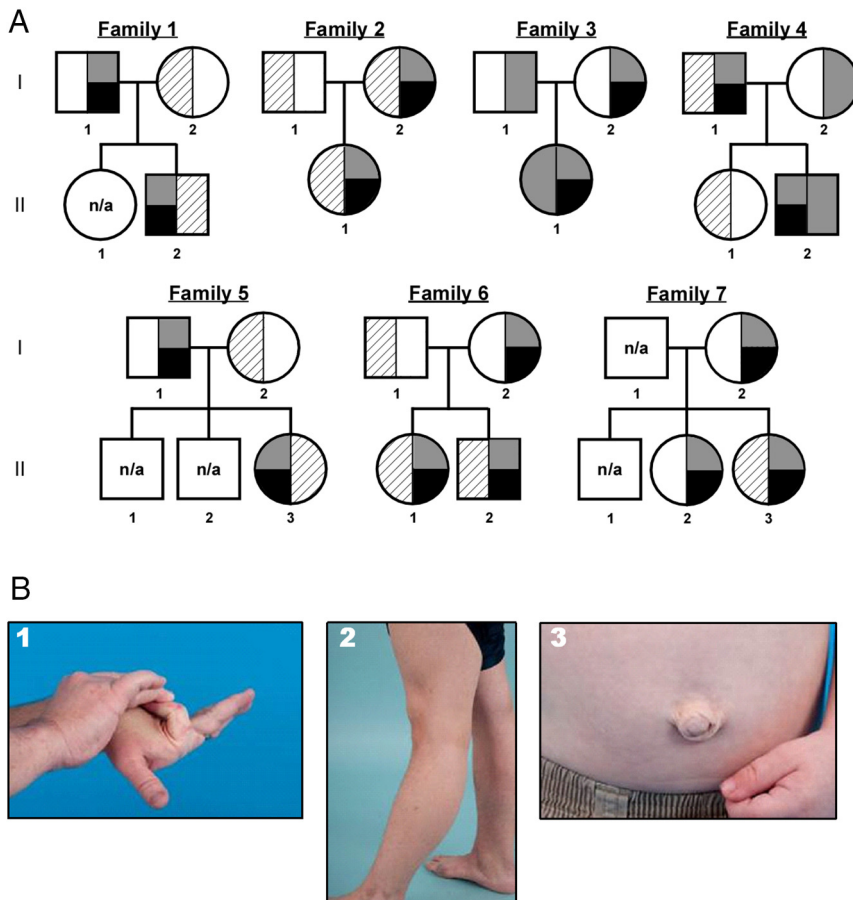
A

B

Figure 1. CAH-X Pedigrees and Clinical Phenotypes. **(A)** The pedigrees of seven novel CAH-X families. Black represents the TNXB C4058W variant. CYP21A2 variants are represented as gray (CYP21A2 deletion due to CYP21A2/CYP21A1P chimera) or striped (other CYP21A2 pathogenic variants). Most CAH patients are compound heterozygotes. Five CAH carrier parents and 1 CAH carrier sibling also have the C4058W mutation. DNA was not available from siblings in Family 1 and 5. **(B)** Clinical findings in patients with CAH-X syndrome due to a C4058W mutation in TNXB. Hypermobile small (1) and large joints (2), and umbilical hernia (3).

phenotype of relatives with the c.12174C>G variant, but not CAH, was less severe, although the majority had hypermobile joints.

To rule out possible pathogenic variants in other known EDS associated genes, we sequenced the *COL3A1, COL5A1,* and *COL5A2* genes in the 10 novel CAH-X patients and found no pathogenic or likely pathogenic variants. Two missense variants of uncertain significance were found in the *COL3A1* gene in patient I-1 from Family 1 and patient II-1 from Family 3. However, these two *COL3A1* variants did not segregate with phenotypes between the parents and the probands, indicating that they are unlikely to be the primary cause of the phenotypes.

c.12174C>G as a Marker of a Novel *TNXA/TNXB* Chimeric Gene

At the locus of *CYP21A2* and *TNXB*, the homology sequence between the pseudo and active *TNX* genes spans the *CYP21A2* 5′ upstream region to intron 31 of *TNXB*; thus, the junction site of a chimeric gene resulting from an

unequal crossover event can vary (**Figure 2A-F**). The reference sequence of the pseudogene *TNXA* (NR_001284.2) at the corresponding c.12174 position is G, suggesting pseudogenic origin of this variation. To test this hypothesis, we sequenced *TNXB* exons 35 through 44 in 11 patients who were previously identified as heterozygous for *TNXA/TNXB* CH-1 (120 bp deletion) because the fragment spanning the exon 35/intron 35 boundary through exon 44 in the *TNXA/TNXB* CH-1 chimera represents the *TNXA*--specific sequence. All 11 patients were heterozygous for c.12174C>G in exon 40; analysis of 7 available parents showed that the 120 bp deletion and the c.12174C>G reside on the same allele (in cis). In addition to c.12174C>G in exon 40, a cluster of three heterozygous variants (c.12218G>A, exon 41; c.12514G>A and c.12524G>A, exon 43) was found in three individuals from two families, Family 3: II-1, Family 4: I-1, and Family 4: II-2 (**Figure 1A, 2G**). Absence of c.12174C>G and these three variants in 100 healthy controls (a subgroup of the 200 controls mentioned above) strongly supports that they are *TNXA*–specific, though only C.12174C>G is likely present in every copy of *TNXA*. Thus, c.12174C>G represents a novel distinguishable site between *TNXA* and *TNXB*.

All of our patients with c.12174C>G had a *CYP21A2* deletion. Most patients (all except Patient II-3 from Family 5) were found to have a *CYP21A1P/CYP21A2* chimera with an undefined junction site downstream of exon 8 (11). Therefore, the junction site of these *CYP21A1P/CYP21A2* chimeras could be located anywhere between intron 8 of *CYP21A2* and intron 35 of *TNXB* representing a contiguous gene deletion of *CYP21A2* and part of *TNXB*. Thus, c.12174C>G can be utilized as a marker of a novel *TNXA/TNXB* chimeric gene. In keeping with the chimeric *CYP21A1P/CYP21A2* gene naming system, (11) we termed the previously identified (120 bp deletion crossing exon 35 and intron 35) and the new (c.12174C>G) *TNXA/TNXB* chimeric genes CAH-X CH-1 and CAH-X CH-2, respectively (**Figure 2E and 2F**). Alternatively, the

Table 1. Clinical Findings in Patients with CAH-X Due to the Novel *TNXB* Variant C4058W

Subject	Sex and Age (yr)	CAH Phenotype	Hyper-mobility Score[a]	Other Joint Findings	Skin Findings	Cardiac Findings	Additional Clinical Features
Family 1: II-2	M/18	SV	4	Multiple subluxations; hypermobile shoulders and feet; hip laxity; chronic arthralgia[b]	Wide scars; striae; skin laxity	Normal	Elongated uvula with midline crease; strabismus; gastroesophageal reflux; hiatal hernia; irritable bowel syndrome; piezogenic papules; bunions; osteopenia
Family 1: I-1	M/49	carrier	3	Hypermobile hands; chronic arthralgia	Skin laxity	Normal	Asthma; hypertension
Family 2: I-2	F/20	NC	5	Chronic arthralgia	Normal	Normal	Scoliosis; gastroesophageal reflux; piezogenic papules
Family 2: II-1	F/45	NC	7	Multiple subluxations; hypermobile shoulders; hip laxity; chronic arthralgia; chronic tendonitis of wrists and knees	Skin laxity	Normal	Umbilical hernia; piezogenic papules
Family 3: II-1	F/6	SW	8	Hip laxity	Normal	Patent foramen ovale until age 4	None
Family 3: I-2	F/43	carrier	1	Hip laxity; torn rotator cuff	Normal	Normal	None
Family 4: II-2	M/2	SW	9	Hip laxity	Skin laxity; doughy skin	Atrial septal aneurysm with patent foramen ovale	Elongated uvula with midline crease; umbilical hernia
Family 4: I-1	M/44	NC	7	Hypermobile hands	Wide scars; congenital third nipple	Mildly enlarged aortic root	Elongated uvula with midline crease; pectus excavatum; varicose veins; chronic plantar fasciitis; pes planus
Family 5: II-3	F/41	SW	6	Shoulder subluxation and bursitis; chronic arthralgia	Striae; skin laxity	Normal	None
Family 5: I-1	M/72	carrier	n/a	Hypermobile shoulders; hip laxity; 2 knee and left shoulder arthroplasties	Normal	Mild RV and LA enlargement; atrial septum aneurysm with patent foramen ovale	Osteoarthritis; spinal stenosis; prostate cancer; epilepsy
Family 6: I-2	F/40	carrier	2	Torn anterior cruciate ligament	Normal	n/a	None
Family 6: II-1	F/13	SW	4	Scoliosis	Normal	Mild partial fusion of the commissure between left and right aortic cusps; mildly dilated aortic root	Turner syndrome; chronic otitis media
Family 6: II-2	M/9	SW	8	Hypermobile hands	Normal	Normal	Chronic urticarial; chronic abdominal pain
Family 7: I-2	F/45	carrier	5	None	Striae	n/a	None
Family 7: II-2	F/17	carrier	6	None	Striae; cystic acne	n/a	None
Family 7: II-3	F/10	NC	5	Rib and elbow subluxations; hypermobile shoulders and hands; hip laxity	Striae	n/a	None

Abbreviations: SW, classic salt-wasting. SV, classic simple-virilizing. NC, non-classic. LV, left ventricle. RV, right ventricle. LA, left atrium. RA, right atrium. n/a, not available. [a]Hypermobility score was assessed by the Beighton scale.**(19)** [b]Arthralgia is at least 3 months duration.

c. 12174C>G variant could be carried over from *TNXA* through a concurrent microgene conversion event instead of a contiguous gene deletion. This likely occurred in Patient II-3 from Family 5 (Table 1), who is compound heterozygous for the *CYP21A1P/CYP21A2* CH-5 chimera (with V281L) and R484P in *CYP21A2*.

The *TNXB* variants identified are located in the fibrinogen, alpha/beta/gamma chain and C-terminal globular domain of the TNX protein. Since c.12174C>G (p.C4058W) was the only variant shared among all probands and affected family members, it is likely pathogenic and suspected to be the primary cause of the phenotypes in these patients.

C4058W Likely Leads to Partial TNX Protein Unfolding

A TNX primary amino acid sequence alignment showed that C4058 is highly conserved within the C-terminal fibrinogen-like domain across mammalian species (**Figure 3A**).

Since a full-length TNX tertiary structure was not available, the TNX C-terminal fibrinogen-like domain (residues 4023–4233) was submitted to the Robetta server for *ab initio* and comparative modeling. The primary protein sequence was first parsed into putative domains (Ginzu), (21) then structural homologs for each domain were identified from protein structural databases and used to build structural models from homology modeling or *ab initio* calculations to predict protein structure (Rosetta) (22, 23).

The Ginzu prediction provided one domain for this region. Rosetta then modeled the domain with high confidence using homology and the known crystal structure for human ficolin-2, a carbohydrate-binding protein with a C-terminal fibrinogen-like domain (PDB: 2J61) (26). The ficolin-2 C-terminal fibrinogen-like domain crystal structure was overlaid with the TNX model (**Figure 3B**, left).

The two structures nicely aligned, supporting the fidelity of this model. A neighboring cysteine in the tertiary structure (position 4028) was predicted to be within disulfide bonding distance of the highly conserved cysteine at position 4058 by three independent university-based online disulfide bonding state predictors (http://bioserv.rpbs.jussieu.fr/cgi-bin/CysState) (24, 25). This predicted disulfide bond is located at the interface between a small segment containing two β-sheets and an alpha helix at the top of the structure and the remaining larger portion of the domain at the bottom, possibly being released and unfolding upon mutation to a tryptophan, resulting in a partially unfolded TNX fibrinogen-like domain (**Figure 3B**, right).

C4058W Disrupts TNX Function but not Expression

In contrast to prior reports of CAH-X CH-1, (8) CAH-X CH-2 dermal fibroblasts did not have altered TNX expression in whole cell lysate compared to CAH controls by western blot (**Figure 3C**). However, CAH-X CH-2 patients had reduced Elastin-Van Gieson histology staining for elastic fibers in dermal biopsies compared to normal controls. Elastin staining in CAH-X CH-1 patients more closely resembled the controls, consistent with prior reports showing a spectrum of elastic fiber abnormalities in TNX haploinsufficient samples (15). Immunohistochemical staining using an antifibrillin-1 antibody showed disrupted fibrillin-1 organization in CAH-X CH-1 and CAH-X CH-2 dermal biopsies compared to normal controls (**Figure 3D**).

CAH-X CH-2 Disrupts the Fibrinogen Domain's Ability to Bind TGF-β1

We hypothesized that CAH-X CH-2 patients may not fully bind TGF-β1 as a consequence of having a mutated fibrinogen-like domain. We coimmunoprecipitated a TNX fragment at the molecular weight of the fibrinogen
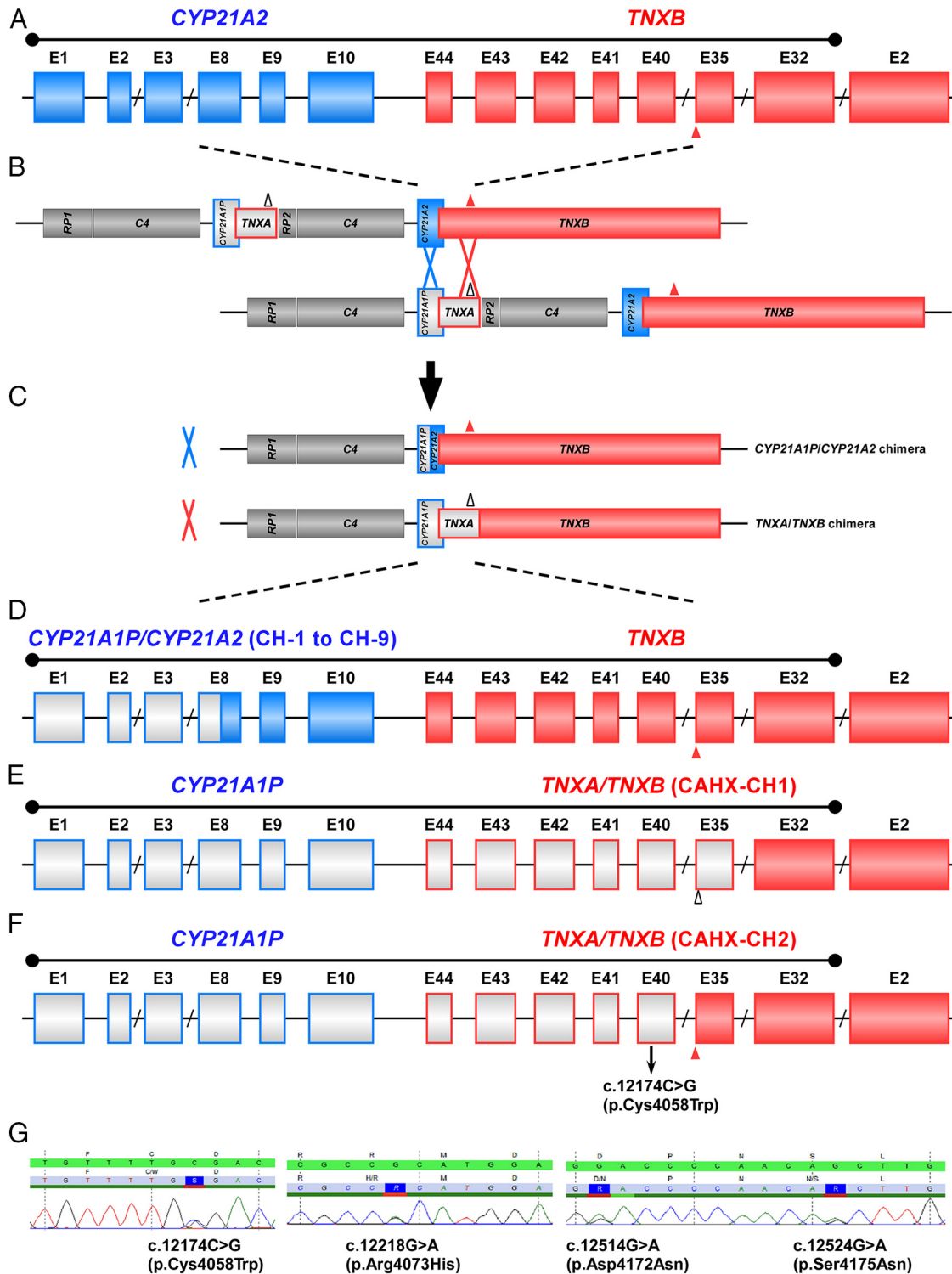
Figure 2. Schematic diagram of CYP21A1P/CYP21A2 and TNXA/TNXB chimera genes. **(A)** Schematic showing exons (rectangles) of the CYP21A2 and TNXB genes. CYP21A2 encodes the active 21-hydroxylase enzyme (blue). TNXB encodes active tenascin-X (red). The sizes of the exons/introns are scaled, with the exception of introns with a slash (eg, CYP21A2 exon 9 is ~100 bp). The homology sequence spans the CYP21A2 5′ upstream region to intron 31 of TNXB. The solid triangle at the boundary of TNXB exon 35 and intron 35 denotes the 120 bp fragment absent in TNXA. **(B)** Unequal crossover during meiosis can occur at the CYP21A2 (blue cross) or TNXB (red cross) locus, resulting in a CYP21A1P/CYP21A2 or TNXA/TNXB chimera. Pseudogenes CYP21A1P and TNXA are in gray and are framed with the color of the corresponding functional gene. RP1 encodes a serine/threonine nuclear kinase (gray), and RP2 is the corresponding truncated pseudogene (gray). C4 encodes the fourth component of serum complement (gray). The open triangle at the boundary of exon 35 and intron 35 denotes the 120 bp deletion in TNXA. **(C)** The CYP21A1P/CYP21A2 and TNXA/TNXB chimeric genes result from unequal crossover. **(D)** Schematic showing exons (rectangles) of a representative CYP21A1P/CYP21A2 chimeric gene (with a junction site in exon 8) and the intact TNXB gene. CYP21A1P/CYP21A2 chimeric genes have been classified into nine types (CH-1 to CH-9) based on the junction site location. **(E)** Schematic showing exons (rectangles) of the

domain using a TGF-β1 antibody in CAH-X CH-2 patient whole cell lysate compared to CAH controls (16). Serum TNX exists as the full-length form, as well as multiple functional fragments, which is also likely reflected at the tissue level (6, 16, 27). Less TNX fragment was pulled down by the TGF-β1 antibody in the CAH-X CH-2 patients compared to CAH controls by western blot, suggesting a disrupted interaction with TGF-β1 (Figure 3E).

Discussion

In this study, we describe increased CAH-X syndrome prevalence relative to our previous report (8) in a large cohort of patients with CAH due to 21-hydroxylase deficiency. Through detailed genetic studies, we identify a pseudogene-derived variant c.12174C>G (p.C4058W) representing a novel *TNXA/TNXB* chimera that does not

---

Legend to Figure 2 Continued. . .

classic TNXA/TNXB chimeric gene with a 120 bp deletion at the boundary of exon 35 and intron 35 (CAHX-CH1). The CYP21A2 gene is completely deleted and replaced by the CYP21A1P pseudogene. **(F)** Schematic showing exons (rectangles) of the newly identified TNXA/TNXB chimeric gene tagged by the c.12174C>G (p.Cys4058Trp) variant in exon 40 (CAHX-CH2). The exon 35 region is intact, while the CYP21A2 gene is completely deleted and replaced by the CYP21A1P pseudogene. **(G)** Sanger sequencing chromatogram of the four variants c.12174C>G (p.Cys4058Trp), c.12218G>A (p.Arg4073His), c.12514G>A (p.Asp4172Asn), and c.12524G>A (p.Ser4175Asn). The green bar is the DNA reference sequence with the encoded amino acids above. The gray bar is the representative patient's DNA sequence with the encoded amino acids above.

Figure 3. Effects of C4058W in the TNX fibrinogen-like domain. **(A)** Primary protein sequence alignment of C4058 in TNX. **(B)** Robetta model of the TNX C-terminal fibrinogen-like domain. Left, Structural overlay of a TNX C-terminal fibrinogen domain model (pink) with the known crystal structure of the highly homologous ficolin-2 C-terminal fibrinogen domain (turquoise, PDB: 2J61 (26)). Right, C4058 is located within probable disulfide bonding distance of C4028 according to disulfide bond state predictor algorithms. **(C)** Representative western blot of TNX expression in CAHX-CH2 patient skin fibroblasts (n = 7) compared to CAH controls (n = 10). Quantification graph includes all patients and controls. TNX expression was normalized to β-tubulin and experiments were done in triplicate. $P \le .05$ considered significant. **(D)** Representative elastin and fibrillin-1 staining in dermal tissue. van Gieson's staining of elastic fibers was reduced (yellow arrows) and immunohistochemical staining showed disorganized fibrillin-1 fibers (black arrows) in both CAHX-CH1 haploinsufficient and CAHX-CH2 patients compared to normal controls. Hematoxylin and eosin were used to counterstain and sections were viewed at 200x magnification. **(E)** Coimmunoprecipitation of the TNX C-terminal fibrinogen domain with TGF-β1. Immunoprecipitations were done using an antihuman TGF-β1 (α-TGF-β1) antibody or control IgG in whole cell lysate from CAHX-CH2 and CAH control fibroblasts. A western blot of the TNX C-terminal fibrinogen domain fragment that was pulled-down is shown. Experiments were done in triplicate.

involve a 120 bp deletion in exon 35. Patients with this novel variant have the cardinal EDS features, such as joint hypermobility and chronic joint pain, as well as midline defects and skin hyperextensibility in a patient subset (8). All patients with CAH-X syndrome described to date have a similar phenotype, disrupted extracellular matrix, and altered TGF-β pathway, although we describe here mutation-specific effects on TNX protein expression (8).

We previously identified CAH-X in 7% of CAH patients; however, the genetic cause underlying the CAH-X phenotype in a patient subgroup was unknown. The lack of unequivocally distinguishable sites between intron 8 of *CYP21* and intron 35 of *TNX* made identification of chimeric gene junction sites challenging. Due to the homologous sequence in this region, an in-depth understanding of the sequence differences between the active genes and pseudogenes is required. Unlike *CYP21A2* and its pseudogene *CYP21A1P*, which have been extensively studied and well characterized, (28) *TNXB* and *TNXA* sequences are still largely unknown. A reference sequence for *TNXA* (NR 001284.2) exists; however, the variations within this pseudogene have never been investigated in detail. In our current study, we utilized the *TNXA*-specific sequence present in the previously identified *TNXA/TNXB* chimera (120 bp deletion in exon 35) to compare with allelic sequences in unaffected controls. *TNXA* and *TNXB* variation profiling and a variant comparison between them in a proper sample size in the general population is essential for future genetic studies of CAH-X and EDS. Cantürk et al showed that *CYP21A1P*-specific variants present with various allele frequencies within *CYP21A1P* (28). Similarly, our data suggest that the c.12174C>G variant is present in every copy of *TNXA*, while the other three identified *TNXA*-specific variants (c.12218G>A, c.12514G>A, and c.12524G>A) may have a lower allele frequency.

The TNX protein is known to regulate collagen deposition and crosslinking, (4, 15, 29) though the mechanism is largely unknown. Recent studies with recombinant TNX constructs and the discovery of a link between TNX and the TGF-β signaling pathway is beginning to elucidate this mechanism. The highly conserved C4058W variant found in this study is located in the fibrinogen-like domain and is likely disulfide bonded, and upon disruption would potentially lead to at least partial protein misfolding and a functional impact. Prior studies of CAH-X and EDS patients carrying the previously identified *TNXA/TNXB* CH-1 gene showed reduced dermal and serum TNX expression compared to controls, supporting a haploinsufficient mechanism (7, 8). However, TNX expression was unchanged in our CAH-X patients carrying the *TNXA/TNXB* CH-2 or *TNXB* variants, suggesting a dominant

negative mechanism. Previous studies showed disrupted elastin fibers and reduced fibrillin-1 staining in patients with autosomal recessive complete TNX deficiency (30) and, to some extent, patients with partial deficiency due to TNX haploinsufficiency (15). Our data revealed reduced elastin staining in dermal biopsies from CAH-X CH-2 patients compared to controls, while the reduction in elastin staining in CAH-X CH-1 samples was less dramatic. Similarly, variable effects of TNX haploinsufficiency on elastin have been reported (15). In our study, fibrillin-1 organization was highly disrupted in all CAH-X patients. Though fibrillin-1 is a part of the elastic fiber and microfibrillar network, it also exists independently and is believed to interact with TNX indirectly to stabilize elastic fiber assembly (30).

TGF-β is known to regulate collagen, (31) and disrupted TGF-β signaling is implicated in a number of connective tissue disorders, (32–36) including CAH-X (17). We previously reported elevated TGF-β biomarkers in both dermal fibroblasts and tissue, as well as in circulation and secreted from cells in patients with CAH-X due to the *TNXA/TNXB* CH-1 chimera (17). We hypothesized that TGF-β pathway disruption could also be responsible for some of the connective tissue phenotypes in our CAH-X CH-2 patients, though likely through a different mechanism. Alcaraz and coworkers showed that the TNX C-terminal fibrinogen-like domain activated the TGF-β pathway by directly interacting with the latent TGF-β complex and inducing a conformational change, causing release of active TGF-β1 and subsequent downstream Smad signaling (16). Similarly, we found that less TNX fibrinogen domain fragment was bound by TGF-β1 in dermal fibroblast whole cell lysate from CAH-X CH-2 patients compared to controls, suggesting a disrupted interaction between TNX and TGF-β1. Further studies are needed to analyze this interaction in CAH-X CH-2 patients.

The clinical impact of carrying a *TNXB* defect includes the risk of chronic joint pain in adulthood, joint subluxations, hernias, and/or organ prolapse, as well as developmental cardiac defects. Unlike previously described patients with CAH-X, several patients with CAH-X due to the novel *TNXA/TNXB* CH-2 had skin laxity with normal healing, reflecting a phenotypic spectrum that may or may not be variant specific. Most hypermobile EDS cases are unexplained (37). Novel ways in which TNX is disrupted, including the novel *TNXA/TNXB* chimera described here, represent potential genetic causes of hypermobile EDS of unknown etiology and requires further study.

A strength of our study is the large cohort size with extensive phenotyping. However, limited sequence infor-

mation on the *TNXA* and *TNXB* genes remains a challenge. Also, the lack of an appropriate CAH-X mouse model is one limitation to fully dissecting the mechanism behind TNX deficiency, though the development of in vitro TNX constructs could address this issue.

Our study shows that multiple *TNXA/TNXB* chimeric genes can lead to CAH-X syndrome, and likely further chimeras remain to be discovered. TNX deficiency effects can be seen through a disrupted ECM and TGF-β signaling pathway in CAH-X patients, though the mechanism behind these effects is likely specific to the nature of the *TNXB* variant. This study reveals novel ways in which connective tissue features can manifest in CAH patients; therefore, more patients may be affected by CAH-X syndrome than previously recognized. We can now estimate that approximately 9% of CAH patients have CAH-X syndrome, expanding the phenotypic spectrum of CAH. Therefore, evaluation for a connective tissue dysplasia is warranted in CAH patients and further studies of *TNXB* may provide insight into the pathogenesis of EDS.

Acknowledgments

References

1. **Merke DP, Bornstein SR.** Congenital adrenal hyperplasia. *Lancet.* 2005;365:2125–2136.
2. **Speiser PW, Azziz R, Baskin LS, Ghizzoni L, Hensle TW, Merke DP, Meyer-Bahlburg HF, Miller WL, Montori VM, Oberfield SE, Ritzen M, White PC, Endocrine S.** Congenital adrenal hyperplasia due to steroid 21-hydroxylase deficiency: an Endocrine Society clinical practice guideline. *The Journal of clinical endocrinology and metabolism.* 2010;95:4133–4160.
3. **Egging D, van Vlijmen-Willems I, van Tongeren T, Schalkwijk J, Peeters A.** Wound healing in tenascin-X deficient mice suggests that tenascin-X is involved in matrix maturation rather than matrix deposition. *Connective tissue research.* 2007;48:93–98.
4. **Mao JR, Taylor G, Dean WB, Wagner DR, Afzal V, Lotz JC, Rubin EM, Bristow J.** Tenascin-X deficiency mimics Ehlers-Danlos syndrome in mice through alteration of collagen deposition. *Nat Genet.* 2002;30:421–425.
5. **Burch GH, Gong Y, Liu W, Dettman RW, Curry CJ, Smith L, Miller WL, Bristow J.** Tenascin-X deficiency is associated with Ehlers-Danlos syndrome. *Nat Genet.* 1997;17:104–108.
6. **Schalkwijk J, Zweers MC, Steijlen PM, Dean WB, Taylor G, van Vlijmen IM, van Haren B, Miller WL, Bristow J.** A recessive form of the Ehlers-Danlos syndrome caused by tenascin-X deficiency. *N Engl J Med.* 2001;345:1167–1175.
7. **Zweers MC, Bristow J, Steijlen PM, Dean WB, Hamel BC, Otero M, Kucharekova M, Boezeman JB, Schalkwijk J.** Haploinsufficiency of TNXB is associated with hypermobility type of Ehlers-Danlos syndrome. *Am J Hum Genet.* 2003;73:214–217.
8. **Merke DP, Chen W, Morissette R, Xu Z, Van Ryzin C, Sachdev V, Hannoush H, Shanbhag SM, Acevedo AT, Nishitani M, Arai AE, McDonnell NB.** Tenascin-X Haploinsufficiency Associated with Ehlers-Danlos Syndrome in Patients with Congenital Adrenal Hyperplasia. *J Clin Endocrinol Metab.* 2013;98:E379–387.
9. **Vrzalova Z, Hruba Z, Hrabincova ES, Vrabelova S, Votava F, Kolouskova S, Fajkusova L.** Chimeric CYP21A1P/CYP21A2 genes identified in Czech patients with congenital adrenal hyperplasia. *European journal of medical genetics.* 2011;54:112–117.
10. **New MI, Abraham M, Gonzalez B, Dumic M, Razzaghy-Azar M, Chitayat D, Sun L, Zaidi M, Wilson RC, Yuen T.** Genotype-phenotype correlation in 1,507 families with congenital adrenal hyperplasia owing to 21-hydroxylase deficiency. *Proceedings of the National Academy of Sciences of the United States of America.* 2013; 110:2611–2616.
11. **Chen W, Xu Z, Sullivan A, Finkielstain GP, Van Ryzin C, Merke DP, McDonnell NB.** Junction site analysis of chimeric CYP21A1P/CYP21A2 genes in 21-hydroxylase deficiency. *Clinical chemistry.* 2012;58:421–430.
12. **Tucker RP, Drabikowski K, Hess JF, Ferralli J, Chiquet-Ehrismann R, Adams JC.** Phylogenetic analysis of the tenascin gene family: evidence of origin early in the chordate lineage. *BMC evolutionary biology.* 2006;6:60.
13. **Gbadegesin RA, Brophy PD, Adeyemo A, Hall G, Gupta IR, Hains D, Bartkowiak B, Rabinovich CE, Chandrasekharappa S, Homstad A, Westreich K, Wu G, Liu Y, Holanda D, Clarke J, Lavin P, Selim A, Miller S, Wiener JS, Ross SS, Foreman J, Rotimi C, Winn MP.** TNXB mutations can cause vesicoureteral reflux. *Journal of the American Society of Nephrology : JASN.* 2013;24:1313–1322.
14. **Penisson-Besnier I, Allamand V, Beurrier P, Martin L, Schalkwijk J, van Vlijmen-Willems I, Gartioux C, Malfait F, Syx D, Macchi L, Marcorelles P, Arbeille B, Croue A, De Paepe A, Dubas F.** Compound heterozygous mutations of the TNXB gene cause primary myopathy. *Neuromuscular disorders : NMD.* 2013;23:664–669.
15. **Zweers MC, Dean WB, van Kuppevelt TH, Bristow J, Schalkwijk J.** Elastic fiber abnormalities in hypermobility type Ehlers-Danlos syndrome patients with tenascin-X mutations. *Clinical genetics.* 2005; 67:330–334.
16. **Alcaraz LB, Exposito JY, Chuvin N, Pommier RM, Cluzel C, Martel S, Sentis S, Bartholin L, Lethias C, Valcourt U.** Tenascin-X promotes epithelial-to-mesenchymal transition by activating latent TGF-beta. *The Journal of cell biology.* 2014;205:409–428.
17. **Morissette R, Merke DP, McDonnell NB.** Transforming growth factor-beta (TGF-beta) pathway abnormalities in tenascin-X deficiency associated with CAH-X syndrome. *European journal of medical genetics.* 2014;57:95–102.
18. **Finkielstain GP, Chen W, Mehta SP, Fujimura FK, Hanna RM, Van Ryzin C, McDonnell NB, Merke DP.** Comprehensive genetic analysis of 182 unrelated families with congenital adrenal hyperplasia due to 21-hydroxylase deficiency. *The Journal of clinical endocrinology and metabolism.* 2011;96:E161–172.
19. **Beighton P, De Paepe A, Steinmann B, Tsipouras P, Wenstrup RJ.** Ehlers-Danlos syndromes: revised nosology, *Villefranche, 1997. Ehlers-Danlos National Foundation (USA) and Ehlers-Danlos Sup-*

port Group (UK). American journal of medical genetics. 1998;77: 31–37.

20. **Ignotz RA, Kelly B, Davis RJ, Massague J.** Biologically active precursor for transforming growth factor type alpha, released by retrovirally transformed cells. *Proceedings of the National Academy of Sciences of the United States of America.* 1986;83:6307–6311.

21. **Kim DE, Chivian D, Malmstrom L, Baker D.** Automated prediction of domain boundaries in CASP6 targets using Ginzu and RosettaDOM. *Proteins.* 2005;61 Suppl 7:193–200.

22. **Simons KT, Kooperberg C, Huang E, Baker D.** Assembly of protein tertiary structures from fragments with similar local sequences using simulated annealing and Bayesian scoring functions. *Journal of molecular biology.* 1997;268:209–225.

23. **Rohl CA, Strauss CE, Chivian D, Baker D.** Modeling structurally variable regions in homologous proteins with rosetta. *Proteins.* 2004;55:656–677.

24. **Ceroni A, Passerini A, Vullo A, Frasconi P.** DISULFIND: a disulfide bonding state and cysteine connectivity prediction server. *Nucleic acids research.* 2006;34:W177–181.

25. **Yaseen A, Li Y.** Dinosolve: a protein disulfide bonding prediction server using context-based features to enhance prediction accuracy. *BMC bioinformatics.* 2013; 14 Suppl 13:S9.

26. **Garlatti V, Martin L, Gout E, Reiser JB, Fujita T, Arlaud GJ, Thielens NM, Gaboriaud C.** Structural basis for innate immune sensing by M-ficolin and its control by a pH-dependent conformational switch. *The Journal of biological chemistry.* 2007;282:35814–35820.

27. **Egging DF, Peeters AC, Grebenchtchikov N, Geurts-Moespot A, Sweep CG, den Heijer M, Schalkwijk J.** Identification and characterization of multiple species of tenascin-X in human serum. *The FEBS journal.* 2007;274:1280–1289.

28. **Canturk C, Baade U, Salazar R, Storm N, Portner R, Hoppner W.** Sequence analysis of CYP21A1P in a German population to aid in the molecular biological diagnosis of congenital adrenal hyperplasia. *Clinical chemistry.* 2011;57:511–517.

29. **Valcourt U, Alcaraz LB, Exposito JY, Lethias C, Bartholin L.** Tenascin-X: beyond the architectural function. *Cell adhesion, migration.* 2015;9:154–165.

30. **Zweers MC, van Vlijmen-Willems IM, van Kuppevelt TH, Mecham RP, Steijlen PM, Bristow J, Schalkwijk J.** Deficiency of tenascin-X

causes abnormalities in dermal elastic fiber morphology. *The Journal of investigative dermatology.* 2004;122:885–891.

31. **Ignotz RA, Massague J.** Transforming growth factor-beta stimulates the expression of fibronectin and collagen and their incorporation into the extracellular matrix. *The Journal of biological chemistry.* 1986;261:4337–4345.

32. **Morissette R, Schoenhoff F, Xu Z, Shilane DA, Griswold BF, Chen W, Yang J, Zhu J, Fert-Bober J, Sloper L, Lehman J, Commins N, Van Eyk JE, McDonnell NB.** Transforming growth factor-beta and inflammation in vascular (type IV) Ehlers-Danlos syndrome. *Circulation Cardiovascular genetics.* 2014;7:80–88.

33. **Doyle AJ, Doyle JJ, Bessling SL, Maragh S, Lindsay ME, Schepers D, Gillis E, Mortier G, Homfray T, Sauls K, Norris RA, Huso ND, Leahy D, Mohr DW, Caulfield MJ, Scott AF, Destree A, Hennekam RC, Arn PH, Curry CJ, Van Laer L, McCallion AS, Loeys BL, Dietz HC.** Mutations in the TGF-beta repressor SKI cause Shprintzen-Goldberg syndrome with aortic aneurysm. *Nature genetics.* 2012; 44:1249–1254.

34. **Habashi JP, Judge DP, Holm TM, Cohn RD, Loeys BL, Cooper TK, Myers L, Klein EC, Liu G, Calvi C, Podowski M, Neptune ER, Halushka MK, Bedja D, Gabrielson K, Rifkin DB, Carta L, Ramirez F, Huso DL, Dietz HC.** Losartan, an AT1 antagonist, prevents aortic aneurysm in a mouse model of Marfan syndrome. *Science.* 2006; 312:117–121.

35. **Lindsay ME, Schepers D, Bolar NA, Doyle JJ, Gallo E, Fert-Bober J, Kempers MJ, Fishman EK, Chen Y, Myers L, Bjeda D, Oswald G, Elias AF, Levy HP, Anderlid BM, Yang MH, Bongers EM, Timmermans J, Braverman AC, Canham N, Mortier GR, Brunner HG, Byers PH, Van Eyk J, Van Laer L, Dietz HC, Loeys BL.** Loss-of-function mutations in TGFB2 cause a syndromic presentation of thoracic aortic aneurysm. *Nature genetics.* 2012;44:922–927.

36. **Loeys BL, Chen J, Neptune ER, Judge DP, Podowski M, Holm T, Meyers J, Leitch CC, Katsanis N, Sharifi N, Xu FL, Myers LA, Spevak PJ, Cameron DE, De Backer J, Hellemans J, Chen Y, Davis EC, Webb CL, Kress W, Coucke P, Rifkin DB, De Paepe AM, Dietz HC.** A syndrome of altered cardiovascular, craniofacial, neurocognitive and skeletal development caused by mutations in TGFBR1 or TGFBR2. *Nature genetics.* 2005;37:275–281.

37. **Colombi M, Dordoni C, Chiarelli N, Ritelli M.** Differential diagnosis and diagnostic flow chart of joint hypermobility syndrome/ehlers-danlos syndrome hypermobility type compared to other heritable connective tissue disorders. *American journal of medical genetics Part C, Seminars in medical genetics.* 2015;169:6–22.